Lepton polarization in $B \to K_1\ell^+\ell^-$ decays

V. Bashiry

Engineering Faculty, Cyprus International University,
Via Mersin 10, Turkey

E-mail: bashiry@ciu.edu.tr

ABSTRACT: We study the single and double lepton polarization asymmetries in the semileptonic B meson decays $B \to K_1(1270)\ell^+\ell^-$ $\ell \equiv e, \mu, \tau)$, where the strange P-wave meson, $K_1(1270)$, is the mixtures of the K_{1A} and K_{1B}, which are the 1^3P_1 and 1^1P_1 states, respectively. The lepton polarization asymmetries show relatively strong dependency in the various region of dileptonic invariant mass. The lepton polarization asymmetries can also be used for determining the $K_1(1270)$–$K_1(1400)$ mixing angle, θ_{K_1} and new physics effects. Furthermore, it is shown that these asymmetries in $B \to K_1(1270)\ell^+\ell^-$ decay compared with those of $B \to K^*\ell^+\ell^-$ decay are more sensitive to the dileptonic invariant mass.

Contents

1 Introduction

The rare flavor-changing neutral-current(FCNC) processes are used to test the predictions of Standard Model(SM) at loop level and for searching new-physics(NP). In this regard, $b \to s(d)$ and $\mu \to e$ transitions have been studied to check predictions of SM at loop level and to look at the NP via their indirect effects where the direct productions are not accessible at present collider experiments. Semileptonic and radiative B decays involving a vector or axial vector meson have been observed by BABAR, BELLE and CLEO. For $B \to K^\star \ell^+ \ell^-$ decays, the forward-backward asymmetry has been measured by BABAR [1] and BELLE [2]. Recently, BABAR [3–5] has reported the measurements for the longitudinal polarization fraction and forward-backward asymmetry (FBA) of $B \to K^*(892)\ell^+\ell^-$, and for the isospin asymmetry of $B^0 \to K^{*0}(892)\ell^+\ell^-$ and $B^\pm \to K^{*\pm}(892)\ell^+\ell^-$ channels. The data may challenge the sings of Wilson coefficients, for instance, C_7^{eff}. In order to extract the magnitudes and arguments of the effective Wilson coefficients, one may measure various observables in various inclusive and exclusive rare processes. In this regrad, the studies of asymmetries, which are less sensitive to the hadronic uncertainties than the branching ratio, are favored. The studies of inclusive and exclusive rare processes as well as various asymmetries should be considerably improved at LHCb. The radiative B decay involving the $K_1(1270)$, the orbitally excited (P-wave) state, is recently observed by Belle and other radiative and semileptonic decay modes involving $K_1(1270)$ and $K_1(1400)$ are hopefully expected to be observed soon. Some studies for $B \to K_1 \ell^+ \ell^-$ involving formfactors, branching ratio and forward-backward(FB) asymmetries of semileptonic decay modes have been made recently [6–9]. In present work, we study the single and double lepton polarization asymmetries in the $B \to K_1(1270)\ell^+\ell^-$ decays. These studies are complimentary to the studies of branching ratio and FB asymmetries. Note that, just like $B \to K^*(892)\ell^+\ell^-$ decays [10–19], $B \to K_1 \ell^+ \ell^-$ decays can be studied for the NP effects, however, these are much more sophisticated due to the mixing of the K_{1A} and K_{1B}, which are the 1^3P_1 and 1^1P_1 states, respectively. The physical K_1 mesons are $K_1(1270)$ and $K_1(1400)$, described

by [9]

$$\begin{pmatrix} |\overline{K}_1(1270)\rangle \\ |\overline{K}_1(1400)\rangle \end{pmatrix} = M \begin{pmatrix} |\overline{K}_{1A}\rangle \\ |\overline{K}_{1B}\rangle \end{pmatrix}, \quad \text{with} \quad M = \begin{pmatrix} \sin\theta_{K_1} & \cos\theta_{K_1} \\ \cos\theta_{K_1} & -\sin\theta_{K_1} \end{pmatrix}. \quad (1.1)$$

The mixing angle θ_{K_1} was estimated to be $|\theta_{K_1}| \approx 34° \vee 57°$ in ref. [20], $35° \leq |\theta_{K_1}| \leq 55°$ in ref. [21], $|\theta_{K_1}| = 37° \vee 58°$ in ref. [22], and $\theta_{K_1} = -(34 \pm 13)°$ in [9, 23]. In this study we will use the results of ref. [9, 23] for numerical calculations.

The paper includes 5 sections: In section 2, we recall the effective Hamiltonian for $B \to K_1(1270)\ell^+\ell^-$ decays. In section 3 we recall the calculations of effective Hamiltonian. In section 4, single and double lepton polarization asymmetries are derived, respectively. In section 5, we examine the sensitivity of these physical observable to the invariant dileptonic mass and our conclusion.

2 The effective Hamiltonian

Using the QCD corrected effective Hamiltonian, the matrix element $b \to s\ell^+\ell^-$ can be written as:

$$M(b \to s\ell^+\ell^-) = \frac{G_F \alpha}{\sqrt{2}\pi} V_{tb} V_{td}^* \left\{ \begin{array}{c} c_9^{\text{eff}} \left[\bar{d}\gamma_\mu L b\right] \left[\bar{\ell}\gamma^\mu \ell\right] \\ +c_{10} \left[\bar{d}\gamma_\mu L b\right] \left[\bar{\ell}\gamma^\mu\gamma^5 \ell\right] \\ -2\hat{m}_b c_7^{\text{eff}} \left[\bar{d}i\sigma_{\mu\nu}\frac{\hat{q}^\nu}{\hat{s}} R b\right] \left[\bar{\ell}\gamma^\mu \ell\right] \end{array} \right\} \quad (2.1)$$

where c_i are Wilson coefficients calculated in naive dimensional regularization (NDR) scheme at the leading order(LO), next to leading order(NLO) and next-to-next leading order (NNLO) in the SM [25]–[32]. $c_9^{\text{eff}}(\hat{s}) = c_9 + Y(\hat{s})$, where $Y(\hat{s}) = Y_{\text{pert}}(\hat{s}) + Y_{\text{LD}}$ contains both the perturbative part $Y_{\text{pert}}(\hat{s})$ and long-distance part $Y_{\text{LD}}(\hat{s})$. $Y(\hat{s})_{\text{pert}}$ is given by [25]

$$\begin{aligned} Y_{\text{pert}}(\hat{s}) =\ & g(\hat{m}_c, \hat{s})c_0 \\ & -\frac{1}{2}g(1, \hat{s})(4\bar{c}_3 + 4\bar{c}_4 + 3\bar{c}_5 + \bar{c}_6) - \frac{1}{2}g(0, \hat{s})(\bar{c}_3 + 3\bar{c}_4) \\ & +\frac{2}{9}(3\bar{c}_3 + \bar{c}_4 + 3\bar{c}_5 + \bar{c}_6), \end{aligned} \quad (2.2)$$

$$\text{with} \quad c_0 \equiv \bar{c}_1 + 3\bar{c}_2 + 3\bar{c}_3 + \bar{c}_4 + 3\bar{c}_5 + \bar{c}_6, \quad (2.3)$$

and the function $g(x, y)$ defined in [25]. Here, $\bar{c}_1$ — $\bar{c}_6$ are the Wilson coefficients in the leading logarithmic approximation. The relevant Wilson coefficients are given in refs. [10]. $Y(\hat{s})_{\text{LD}}$ involves $B \to K_1 V(\bar{c}c)$ resonances [26, 33, 34], where $V(\bar{c}c)$ are the vector charmonium states. We follow refs. [26, 33] and set

$$Y_{\text{LD}}(\hat{s}) = -\frac{3\pi}{\alpha_{\text{em}}^2} c_0 \sum_{V=\psi(1s),...} \kappa_V \frac{\hat{m}_V \mathcal{B}(V \to \ell^+\ell^-)\hat{\Gamma}_{\text{tot}}^V}{\hat{s} - \hat{m}_V^2 + i\hat{m}_V\hat{\Gamma}_{\text{tot}}^V}, \quad (2.4)$$

V	Mass[GeV]	Γ_{tot}^V[MeV]	$\mathcal{B}(V \to \ell^+\ell^-)$	
$J/\Psi(1S)$	3.097	0.093	5.9×10^{-2}	for $\ell = e, \mu$
$\Psi(2S)$	3.686	0.327	7.4×10^{-3}	for $\ell = e, \mu$
			3.0×10^{-3}	for $\ell = \tau$
$\Psi(3770)$	3.772	25.2	9.8×10^{-6}	for $\ell = e$
$\Psi(4040)$	4.040	80	1.1×10^{-5}	for $\ell = e$
$\Psi(4160)$	4.153	103	8.1×10^{-6}	for $\ell = e$
$\Psi(4415)$	4.421	62	9.4×10^{-6}	for $\ell = e$

Table 1. Masses, total decay widths and branching fractions of dilepton decays of vector charmonium states [24].

where $\hat{\Gamma}_{\text{tot}}^V \equiv \Gamma_{\text{tot}}^V/m_B$ and κ_V takes different value for different exclusive semileptonic decay. This phenomenological parameters κ_V can be fixed for $B \to K^*\ell^+\ell^-$ decay by equating the naive factorization estimate of the $B \to K^*V$ rate and the experimental measured results [10]. Except for the branching ratio of $B \to J/\Psi K_1(1270)$ [24], there is no experimental results on $B \to K_1 V(c\bar{c})$. Thus, we will use the results of $B \to K^*V$ to estimate the values of κ_V. We assume that the effect of substituting K^* with K_1 is identical in the radiative and in the non leptonic decay, in other words that each form factor for the $B \to K_1$ transition is given by the corresponding form factor for $B \to K^*$ multiplied by the same factor y, which is define as follows [35]:

$$y = \frac{f^{B \to K_1}(0)}{f^{B \to K^*}(0)} \approx 1.06 \tag{2.5}$$

once the change of parity between the two strange mesons is taken into account. We predict that

$$\kappa_V(B \to K_1) \approx 1.06 \ \kappa_V(B \to K^*) \tag{2.6}$$

. Using the above equation and the results for κ_V obtained for $B \to K^*$ transition [10]. We find $\kappa_V = 1.75$ for $J/\Psi(1S)$ and $\kappa_V = 2.43$ for $\Psi(2S)$, respectively. The relevant properties of vector charmonium states are summarized in table 1.

The matrix element for the exclusive decay can be obtain by sandwiching eq. (2.1) between initial hadron state $B(p_B)$ and final hadron state K_1 in terms of formfactors.

The $\overline{B}(p_B) \to \overline{K}_1(p_{K_1}, \lambda)$ formfactors are defined as (see [9])

$$\langle \overline{K}_1(p_{K_1}, \lambda)|\bar{s}\gamma_\mu(1 - \gamma_5)b|\overline{B}(p_B)\rangle$$
$$= -i\frac{2}{m_B + m_{K_1}}\epsilon_{\mu\nu\rho\sigma}\varepsilon_{(\lambda)}^{*\nu}p_B^\rho p_{K_1}^\sigma A^{K_1}(q^2)$$
$$- \left[(m_B + m_{K_1})\varepsilon_\mu^{(\lambda)*}V_1^{K_1}(q^2) - (p_B + p_{K_1})_\mu(\varepsilon_{(\lambda)}^* \cdot p_B)\frac{V_2^{K_1}(q^2)}{m_B + m_{K_1}}\right]$$
$$+ 2m_{K_1}\frac{\varepsilon_{(\lambda)}^* \cdot p_B}{q^2}q_\mu\left[V_3^{K_1}(q^2) - V_0^{K_1}(q^2)\right], \tag{2.7}$$

– 3 –

$$\langle \overline{K}_1(p_{K_1}, \lambda) | \bar{s}\sigma_{\mu\nu} q^\nu (1+\gamma_5) b | \overline{B}(p_B) \rangle$$
$$= 2 T_1^{K_1}(q^2) \epsilon_{\mu\nu\rho\sigma} \varepsilon_{(\lambda)}^{*\nu} p_B^\rho p_{K_1}^\sigma$$
$$- i T_2^{K_1}(q^2) \left[(m_B^2 - m_{K_1}^2) \varepsilon_{*\mu}^{(\lambda)} - (\varepsilon_{(\lambda)}^* \cdot q)(p_B + p_{K_1})_\mu \right]$$
$$- i T_3^{K_1}(q^2)(\varepsilon_{(\lambda)}^* \cdot q) \left[q_\mu - \frac{q^2}{m_B^2 - m_{K_1}^2}(p_{K_1} + p_B)_\mu \right], \tag{2.8}$$

where $q \equiv p_B - p_{K_1} = p_{\ell^+} + p_{\ell^-}$. In order to ensure finiteness at $q^2 = 0$, it is required

$$V_3^{K_1}(0) = V_0^{K_1}(0), \quad T_1^{K_1}(0) = T_2^{K_1}(0),$$
$$V_3^{K_1}(q^2) = \frac{m_B + m_{K_1}}{2 m_{K_1}} V_1^{K_1}(q^2) - \frac{m_B - m_{K_1}}{2 m_{K_1}} V_2^{K_1}(q^2). \tag{2.9}$$

The formfactors of $B \to K_1(1270)$ and $B \to K_1(1400)$ can be expressed in terms of $B \to K_A$ and $B \to K_B$ as follows(see [9]):

$$\begin{pmatrix} \langle \overline{K}_1(1270) | \bar{s}\gamma_\mu(1-\gamma_5)b | \overline{B} \rangle \\ \langle \overline{K}_1(1400) | \bar{s}\gamma_\mu(1-\gamma_5)b | \overline{B} \rangle \end{pmatrix} = M \begin{pmatrix} \langle \overline{K}_{1A} | \bar{s}\gamma_\mu(1-\gamma_5)b | \overline{B} \rangle \\ \langle \overline{K}_{1B} | \bar{s}\gamma_\mu(1-\gamma_5)b | \overline{B} \rangle \end{pmatrix}, \tag{2.10}$$

$$\begin{pmatrix} \langle \overline{K}_1(1270) | \bar{s}\sigma_{\mu\nu}q^\nu(1+\gamma_5)b | \overline{B} \rangle \\ \langle \overline{K}_1(1400) | \bar{s}\sigma_{\mu\nu}q^\nu(1+\gamma_5)b | \overline{B} \rangle \end{pmatrix} = M \begin{pmatrix} \langle \overline{K}_{1A} | \bar{s}\sigma_{\mu\nu}q^\nu(1+\gamma_5)b | \overline{B} \rangle \\ \langle \overline{K}_{1B} | \bar{s}\gamma_{\mu\nu}q^\nu(1+\gamma_5)b | \overline{B} \rangle \end{pmatrix}, \tag{2.11}$$

using the mixing matrix M being given in eq. (1.1) the formfactors $A^{K_1}, V_{0,1,2}^{K_1}$ and $T_{1,2,3}^{K_1}$ can be written as follows:

$$\begin{pmatrix} A^{K_1(1270)}/(m_B + m_{K_1(1270)}) \\ A^{K_1(1400)}/(m_B + m_{K_1(1400)}) \end{pmatrix} = M \begin{pmatrix} A^{K_{1A}}/(m_B + m_{K_{1A}}) \\ A^{K_{1B}}/(m_B + m_{K_{1B}}) \end{pmatrix}, \tag{2.12}$$

$$\begin{pmatrix} (m_B + m_{K_1(1270)}) V_1^{K_1(1270)} \\ (m_B + m_{K_1(1400)}) V_1^{K_1(1400)} \end{pmatrix} = M \begin{pmatrix} (m_B + m_{K_{1A}}) V_1^{K_{1A}} \\ (m_B + m_{K_{1B}}) V_1^{K_{1B}} \end{pmatrix}, \tag{2.13}$$

$$\begin{pmatrix} V_2^{K_1(1270)}/(m_B + m_{K_1(1270)}) \\ V_2^{K_1(1400)}/(m_B + m_{K_1(1400)}) \end{pmatrix} = M \begin{pmatrix} V_2^{K_{1A}}/(m_B + m_{K_{1A}}) \\ V_2^{K_{1B}}/(m_B + m_{K_{1B}}) \end{pmatrix}, \tag{2.14}$$

$$\begin{pmatrix} m_{K_1(1270)} V_0^{K_1(1270)} \\ m_{K_1(1400)} V_0^{K_1(1400)} \end{pmatrix} = M \begin{pmatrix} m_{K_{1A}} V_0^{K_{1A}} \\ m_{K_{1B}} V_0^{K_{1B}} \end{pmatrix}, \tag{2.15}$$

$$\begin{pmatrix} T_1^{K_1(1270)} \\ T_1^{K_1(1400)} \end{pmatrix} = M \begin{pmatrix} T_1^{K_{1A}} \\ T_1^{K_{1B}} \end{pmatrix}, \tag{2.16}$$

$$\begin{pmatrix} (m_B^2 - m_{K_1(1270)}^2) T_2^{K_1(1270)} \\ (m_B^2 - m_{K_1(1400)}^2) T_2^{K_1(1400)} \end{pmatrix} = M \begin{pmatrix} (m_B^2 - m_{K_{1A}}^2) T_2^{K_{1A}} \\ (m_B^2 - m_{K_{1B}}^2) T_2^{K_{1B}} \end{pmatrix}, \tag{2.17}$$

$$\begin{pmatrix} T_3^{K_1(1270)} \\ T_3^{K_1(1400)} \end{pmatrix} = M \begin{pmatrix} T_3^{K_{1A}} \\ T_3^{K_{1B}} \end{pmatrix}, \tag{2.18}$$

where it is supposed that $p_{K_1(1270),K_1(1400)}^\mu \simeq p_{K_{1A}}^\mu \simeq p_{K_{1B}}^\mu$ [9]. These formfactors within light-cone sum rule (LCSR) are estimated in [36]. The momentum dependence of all

formfactors is parameterized as:

$$F(q^2) = \frac{F(0)}{1 - a(q^2/m_B^2) + b(q^2/m_B^2)^2}. \tag{2.19}$$

The values of $F(0)$, a and b parameters are exhibited in table 2.

Thus, the matrix element for $B \to K_1 \ell^+ \ell^-$ in terms of formfactos is given by

$$\mathcal{M} = \frac{G_F \alpha_{\rm em}}{2\sqrt{2}\pi} V_{ts}^* V_{tb} \, m_B \cdot (-i) \left[\mathcal{T}_\mu^{(K_1),1} \bar{\ell} \gamma^\mu \ell + \mathcal{T}_\mu^{(K_1),2} \bar{\ell} \gamma^\mu \gamma_5 \ell \right], \tag{2.20}$$

where

$$\begin{aligned}
\mathcal{T}_\mu^{(K_1),1} &= \mathcal{A}^{K_1}(\hat{s}) \epsilon_{\mu\nu\rho\sigma} \varepsilon^{*\nu} \hat{p}_B^\rho \hat{p}_{K_1}^\sigma - i\mathcal{B}^{K_1}(\hat{s}) \varepsilon_\mu^* \\
&\quad + i\mathcal{C}^{K_1}(\hat{s})(\varepsilon^* \cdot \hat{p}_B) \hat{p}_\mu + i\mathcal{D}^{K_1}(\hat{s})(\varepsilon^* \cdot \hat{p}_B) \hat{q}_\mu, \tag{2.21}
\end{aligned}$$

$$\begin{aligned}
\mathcal{T}_\mu^{(K_1),2} &= \mathcal{E}^{K_1}(\hat{s}) \epsilon_{\mu\nu\rho\sigma} \varepsilon^{*\nu} \hat{p}_B^\rho \hat{p}_{K_1}^\sigma - i\mathcal{F}^{K_1}(\hat{s}) \varepsilon_\mu^* \\
&\quad + i\mathcal{G}^{K_1}(\hat{s})(\varepsilon^* \cdot \hat{p}_B) \hat{p}_\mu + i\mathcal{H}^{K_1}(\hat{s})(\varepsilon^* \cdot \hat{p}_B) \hat{q}_\mu, \tag{2.22}
\end{aligned}$$

with $\hat{p} = p/m_B$, $\hat{p}_B = p_B/m_B$, $\hat{q} = q/m_B$ and $p = p_B + p_{K_1}$, $q = p_B - p_{K_1} = p_{\ell^+} + p_{\ell^-}$.

Here $\mathcal{A}^{K_1}(\hat{s}), \ldots, \mathcal{H}^{K_1}(\hat{s})$ are defined by

$$\mathcal{A}^{K_1}(\hat{s}) = \frac{2}{1 + \sqrt{\hat{r}_{K_1}}} c_9^{\rm eff}(\hat{s}) A^{K_1}(\hat{s}) + \frac{4\hat{m}_b}{\hat{s}} c_7^{\rm eff} T_1^{K_1}(\hat{s}), \tag{2.23}$$

$$\mathcal{B}^{K_1}(\hat{s}) = \left(1 + \sqrt{\hat{r}_{K_1}}\right) \left[c_9^{\rm eff}(\hat{s}) V_1^{K_1}(\hat{s}) + \frac{2\hat{m}_b}{\hat{s}} \left(1 - \sqrt{\hat{r}_{K_1}}\right) c_7^{\rm eff} T_2^{K_1}(\hat{s}) \right], \tag{2.24}$$

$$\mathcal{C}^{K_1}(\hat{s}) = \frac{1}{1 - \hat{r}_{K_1}} \left[\left(1 - \sqrt{\hat{r}_{K_1}}\right) c_9^{\rm eff}(\hat{s}) V_2^{K_1}(\hat{s}) + 2\hat{m}_b c_7^{\rm eff} \left(T_3^{K_1}(\hat{s}) + \frac{1 - \sqrt{\hat{r}_{K_1}}^2}{\hat{s}} T_2^{K_1}(\hat{s}) \right) \right], \tag{2.25}$$

$$\begin{aligned}
\mathcal{D}^{K_1}(\hat{s}) &= \frac{1}{\hat{s}} \Big[c_9^{\rm eff}(\hat{s}) \left\{ \left(1 + \sqrt{\hat{r}_{K_1}}\right) V_1^{K_1}(\hat{s}) - \left(1 - \sqrt{\hat{r}_{K_1}}\right) V_2^{K_1}(\hat{s}) - 2\sqrt{\hat{r}_{K_1}} V_0^{K_1}(\hat{s}) \right\} \\
&\quad - 2\hat{m}_b c_7^{\rm eff} T_3^{K_1}(\hat{s}) \Big], \tag{2.26}
\end{aligned}$$

$$\mathcal{E}^{K_1}(\hat{s}) = \frac{2}{1 + \sqrt{\hat{r}_{K_1}}} c_{10} A^{K_1}(\hat{s}), \tag{2.27}$$

$$\mathcal{F}^{K_1}(\hat{s}) = \left(1 + \sqrt{\hat{r}_{K_1}}\right) c_{10} V_1^{K_1}(\hat{s}), \tag{2.28}$$

$$\mathcal{G}^{K_1}(\hat{s}) = \frac{1}{1 + \sqrt{\hat{r}_{K_1}}} c_{10} V_2^{K_1}(\hat{s}), \tag{2.29}$$

$$\mathcal{H}^{K_1}(\hat{s}) = \frac{1}{\hat{s}} c_{10} \left[\left(1 + \sqrt{\hat{r}_{K_1}}\right) V_1^{K_1}(\hat{s}) - \left(1 - \sqrt{\hat{r}_{K_1}}\right) V_2^{K_1}(\hat{s}) - 2\sqrt{\hat{r}_{K_1}} V_0^{K_1}(\hat{s}) \right], \tag{2.30}$$

with $\hat{r}_{K_1} = m_{K_1}^2/m_B^2$, $\hat{m}_\ell = m_\ell/m_B$ and $\hat{s} = q^2/m_B^2$. The differential decay spectrum can be obtained from the decay amplitude

$$\frac{d\Gamma(\overline{B} \to \overline{K}_1 \ell^+ \ell^-)}{d\hat{s}} = \frac{G_F^2 \alpha_{\rm em}^2 m_B^5}{2^8 \pi^5} |V_{tb} V_{ts}^*|^2 \, v\sqrt{\lambda} \Delta(\hat{s}) \tag{2.31}$$

F	$F(0)$	a	b	F	$F(0)$	a	b
$V_1^{BK_{1A}}$	0.34 ± 0.07	0.635	0.211	$V_1^{BK_{1B}}$	$-0.29^{+0.08}_{-0.05}$	0.729	0.074
$V_2^{BK_{1A}}$	0.41 ± 0.08	1.51	1.18	$V_2^{BK_{1B}}$	$-0.17^{+0.05}_{-0.03}$	0.919	0.855
$V_0^{BK_{1A}}$	0.22 ± 0.04	2.40	1.78	$V_0^{BK_{1B}}$	$-0.45^{+0.12}_{-0.08}$	1.34	0.690
$A^{BK_{1A}}$	0.45 ± 0.09	1.60	0.974	$A^{BK_{1B}}$	$-0.37^{+0.10}_{-0.06}$	1.72	0.912
$T_1^{BK_{1A}}$	$0.31^{+0.09}_{-0.05}$	2.01	1.50	$T_1^{BK_{1B}}$	$-0.25^{+0.06}_{-0.07}$	1.59	0.790
$T_2^{BK_{1A}}$	$0.31^{+0.09}_{-0.05}$	0.629	0.387	$T_2^{BK_{1B}}$	$-0.25^{+0.06}_{-0.07}$	0.378	-0.755
$T_3^{BK_{1A}}$	$0.28^{+0.08}_{-0.05}$	1.36	0.720	$T_3^{BK_{1B}}$	-0.11 ± 0.02	-1.61	10.2

Table 2. Formfactors for $B \to K_{1A}, K_{1B}$ transitions obtained in the LCSR calculation [36] are fitted to the 3-parameter form in eq. (2.19).

$$
\Delta = \frac{8 Re[\mathcal{F}\mathcal{H}^*]\hat{m}_\ell^2 \lambda}{\hat{r}_{K_1}} + \frac{8 Re[\mathcal{G}\mathcal{H}^*]\hat{m}_\ell^2(-1+\hat{r}_{K_1})\lambda}{\hat{r}_{K_1}} - \frac{8|\mathcal{H}|^2 \hat{m}_\ell^2 \hat{s} \lambda}{\hat{r}_{K_1}}
$$
$$
- \frac{2 Re[\mathcal{B}\mathcal{C}^*](-1+\hat{r}_{K_1}+\hat{s})(3+3\hat{r}_{K_1}^2-6\hat{s}+3\hat{s}^2-6\hat{r}_{K_1}(1+\hat{s})-v^2\lambda)}{3\hat{r}_{K_1}}
$$
$$
- \frac{|\mathcal{C}|^2 \lambda(3+3\hat{r}_{K_1}^2-6\hat{s}+3\hat{s}^2-6\hat{r}_{K_1}(1+\hat{s})-v^2\lambda)}{3\hat{r}_{K_1}}
$$
$$
- \frac{|\mathcal{G}|^2 \lambda(3+3\hat{r}_{K_1}^2+12\hat{m}_\ell^2(2+2\hat{r}_{K_1}-\hat{s})-6\hat{s}+3\hat{s}^2-6\hat{r}_{K_1}(1+\hat{s})-v^2\lambda)}{3\hat{r}_{K_1}}
$$
$$
+ \frac{|\mathcal{F}|^2(-3-3\hat{r}_{K_1}^2+6\hat{r}_{K_1}(1+16\hat{m}_\ell^2-3\hat{s})+6\hat{s}-3\hat{s}^2+v^2\lambda)}{3\hat{r}_{K_1}}
$$
$$
+ \frac{|\mathcal{B}|^2(-3-3\hat{r}_{K_1}^2+6\hat{s}-3\hat{s}^2-6\hat{r}_{K_1}(-1+8\hat{m}_\ell^2+3\hat{s})+v^2\lambda)}{3\hat{r}_{K_1}}
$$
$$
+ \frac{2}{3\hat{r}_{K_1}} Re[\mathcal{F}\mathcal{G}^*](12\hat{m}_\ell^2\lambda-(-1+\hat{r}_{K_1}+\hat{s})(3+3\hat{r}_{K_1}^2-6\hat{s}+3\hat{s}^2-6\hat{r}_{K_1}(1+\hat{s})-v^2\lambda))
$$
$$
+ |\mathcal{A}|^2 \left(-4\hat{m}_\ell^2\lambda - \frac{\hat{s}}{3}\left(3+3\hat{r}_{K_1}^2-6\hat{s}+3\hat{s}^2-6\hat{r}_{K_1}(1+\hat{s})+v^2\lambda\right) \right)
$$
$$
+ |\mathcal{E}|^2 \left(4\hat{m}_\ell^2\lambda - \frac{\hat{s}}{3}\left(3+3\hat{r}_{K_1}^2-6\hat{s}+3\hat{s}^2-6\hat{r}_{K_1}(1+\hat{s})+v^2\lambda\right) \right)
$$

3 Lepton polarization asymmetries

In order to calculate the polarization asymmetries of the leptons, we must first define the orthogonal vectors S in the rest frame of ℓ^- and W in the rest frame of ℓ^+ (where these vectors are the polarization vectors of the leptons). Note that, we will use the subscripts L, N and T to correspond to the leptons which are polarized along with the longitudinal, normal and transverse polarization of leptons, respectively. [34, 37].

$$
S_L^\mu \equiv (0, \mathbf{e}_L) = \left(0, \frac{\mathbf{p}_-}{|\mathbf{p}_-|} \right),
$$
$$
S_N^\mu \equiv (0, \mathbf{e}_N) = \left(0, \frac{\mathbf{p}_{K_1} \times \mathbf{p}_-}{|\mathbf{p}_{K_1} \times \mathbf{p}_-|} \right),
$$

$$S_T^\mu \equiv (0, \mathbf{e}_T) = (0, \mathbf{e}_N \times \mathbf{e}_L), \tag{3.1}$$

$$W_L^\mu \equiv (0, \mathbf{w}_L) = \left(0, \frac{\mathbf{p}_+}{|\mathbf{p}_+|}\right),$$

$$W_N^\mu \equiv (0, \mathbf{w}_N) = \left(0, \frac{\mathbf{p}_{K_1} \times \mathbf{p}_+}{|\mathbf{p}_{K_1} \times \mathbf{p}_+|}\right),$$

$$W_T^\mu \equiv (0, \mathbf{w}_T) = (0, \mathbf{w}_N \times \mathbf{w}_L), \tag{3.2}$$

where $\mathbf{p}_+$, $\mathbf{p}_-$ and $\mathbf{p}_{K_1}$ are the three momenta of the ℓ^+, ℓ^- and K_1 particles, respectively. On boosting the vectors defined by eqs. (3.1), (3.2) to the CM frame of the $\ell^- \ell^+$ system only the longitudinal vector will be boosted, while the other two remain the same. The longitudinal vectors in the CM frame of the $\ell^- \ell^+$ system become;

$$S_L^\mu = \left(\frac{|\mathbf{p}_-|}{m_\ell}, \frac{E_\ell \mathbf{p}_-}{m_\ell |\mathbf{p}_-|}\right),$$

$$W_L^\mu = \left(\frac{|\mathbf{p}_-|}{m_\ell}, -\frac{E_\ell \mathbf{p}_-}{m_\ell |\mathbf{p}_-|}\right). \tag{3.3}$$

The polarization asymmetries can now be calculated using the spin projector $\frac{1}{2}(1 + \gamma_5 \rlap{/}{S})$ for ℓ^- and the spin projector $\frac{1}{2}(1 + \gamma_5 \rlap{/}{W})$ for ℓ^+. The single and double-lepton polarization asymmetries P_{ij} are defined, respectively, as [37]

$$P_i = \frac{\frac{d\Gamma(\mathbf{s}^\pm = \hat{\mathbf{i}})}{d\hat{s}} - \frac{d\Gamma(\mathbf{s}^\pm = -\hat{\mathbf{i}})}{d\hat{s}}}{\frac{d\Gamma(\mathbf{s}^\pm = \hat{\mathbf{i}})}{d\hat{s}} + \frac{d\Gamma(\mathbf{s}^\pm = -\hat{\mathbf{i}})}{d\hat{s}}} \tag{3.4}$$

and

$$P_{ij} = \frac{\left[\frac{d\Gamma(\mathbf{s}^+ = \hat{\mathbf{i}}, \mathbf{s}^- = \hat{\mathbf{j}})}{d\hat{s}} - \frac{d\Gamma(\mathbf{s}^+ = \hat{\mathbf{i}}, \mathbf{s}^- = -\hat{\mathbf{j}})}{d\hat{s}}\right] - \left[\frac{d\Gamma(\mathbf{s}^+ = -\hat{\mathbf{i}}, \mathbf{s}^- = \hat{\mathbf{j}})}{d\hat{s}} - \frac{d\Gamma(\mathbf{s}^+ = -\hat{\mathbf{i}}, \mathbf{s}^- = -\hat{\mathbf{j}})}{d\hat{s}}\right]}{\left[\frac{d\Gamma(\mathbf{s}^+ = \hat{\mathbf{i}}, \mathbf{s}^- = \hat{\mathbf{j}})}{d\hat{s}} + \frac{d\Gamma(\mathbf{s}^+ = \hat{\mathbf{i}}, \mathbf{s}^- = -\hat{\mathbf{j}})}{d\hat{s}}\right] + \left[\frac{d\Gamma(\mathbf{s}^+ = -\hat{\mathbf{i}}, \mathbf{s}^- = \hat{\mathbf{j}})}{d\hat{s}} + \frac{d\Gamma(\mathbf{s}^+ = -\hat{\mathbf{i}}, \mathbf{s}^- = -\hat{\mathbf{j}})}{d\hat{s}}\right]}, \tag{3.5}$$

where $\hat{i} = L, N, T$ and $\hat{j} = L, N, T$ are unit vectors.

Equipped with these definitions, we evaluate the single and double lepton polarization asymmetries and obtain the following results:

$$P_L = -\frac{2Re[\mathcal{B}\mathcal{G}^*](\hat{r}_{K_1} + \hat{s} - 1)v\left(3\hat{r}_{K_1}^2 - 6(\hat{s}+1)\hat{r}_{K_1} + 3(\hat{s}-1)^2 - \lambda\right)}{3\hat{r}_{K_1}}$$

$$-\frac{2Re[\mathcal{C}\mathcal{F}^*](\hat{r}_{K_1} + \hat{s} - 1)v\left(3\hat{r}_{K_1}^2 - 6(\hat{s}+1)\hat{r}_{K_1} + 3(\hat{s}-1)^2 - \lambda\right)}{3\hat{r}_{K_1}}$$

$$-\frac{2Re[\mathcal{C}\mathcal{G}^*]v\lambda\left(3\hat{r}_{K_1}^2 - 6(\hat{s}+1)\hat{r}_{K_1} + 3(\hat{s}-1)^2 - \lambda\right)}{3\hat{r}_{K_1}}$$

$$-\frac{2}{3}Re[\mathcal{A}\mathcal{E}^*]\hat{s}v\left(3\hat{r}_{K_1}^2 - 6(\hat{s}+1)\hat{r}_{K_1} + 3(\hat{s}-1)^2 + \lambda\right)$$

$$+\frac{2Re[\mathcal{B}\mathcal{F}^*]v\left(\lambda - 3\left(\hat{r}_{K_1}^2 + (6\hat{s}-2)\hat{r}_{K_1} + (\hat{s}-1)^2\right)\right)}{3\hat{r}_{K_1}} \tag{3.6}$$

$$P_T = \pi\hat{m}_\ell\sqrt{\lambda}\Bigg\{ -\frac{Re[\mathcal{CH}^*]\sqrt{\hat{s}}\lambda}{\hat{r}_{K_1}} + \frac{Re[\mathcal{CF}^*]\lambda}{\hat{r}_{K_1}\sqrt{\hat{s}}} + \frac{Re[\mathcal{CG}^*](\hat{r}_{K_1}-1)\lambda}{\hat{r}_{K_1}\sqrt{\hat{s}}}$$

$$-\frac{Re[\mathcal{BH}^*]\sqrt{\hat{s}}(\hat{r}_{K_1}+\hat{s}-1)}{\hat{r}_{K_1}} + \frac{Re[\mathcal{BF}^*](\hat{r}_{K_1}+\hat{s}-1)}{\hat{r}_{K_1}\sqrt{\hat{s}}}$$

$$+\frac{Re[\mathcal{BG}^*](\hat{r}_{K_1}-1)(\hat{r}_{K_1}+\hat{s}-1)}{\hat{r}_{K_1}\sqrt{\hat{s}}} - 4Re[\mathcal{AB}^*]\sqrt{\hat{s}}\Bigg\}$$

$$P_N = i\pi\hat{m}_\ell\sqrt{\lambda}\Bigg\{ \frac{Im[\mathcal{GH}^*]\sqrt{\hat{s}}\lambda}{\hat{r}_{K_1}} + \frac{Im[\mathcal{FG}^*]\sqrt{\hat{s}}(-3\hat{r}_{K_1}+\hat{s}-1)}{\hat{r}_{K_1}} \tag{3.7}$$

$$+\frac{Im[\mathcal{FH}^*]\sqrt{\hat{s}}(\hat{r}_{K_1}+\hat{s}-1)}{\hat{r}_{K_1}} - 2Im[\mathcal{AF}^*]\sqrt{\hat{s}} - 2Im[\mathcal{AE}^*]\sqrt{\hat{s}}\Bigg\}$$

$$P_{LL} = \frac{4Re[\mathcal{FH}^*](2\hat{m}_\ell^2+\hat{s})\lambda}{\hat{r}_{K_1}} + \frac{4Re[\mathcal{GH}^*](-1+\hat{r}_{K_1})(2\hat{m}_\ell^2+\hat{s})\lambda}{\hat{r}_{K_1}}$$

$$-\frac{2|\mathcal{H}|^2\hat{s}(2\hat{m}_\ell^2+\hat{s})\lambda}{\hat{r}_{K_1}} - \frac{|\mathcal{G}|^2}{6\hat{m}_\ell^2\hat{r}_{K_1}\hat{s}}\Bigg(\hat{s}^2(3\hat{r}_{K_1}^2+3(-1+\hat{s})^2-6\hat{r}_{K_1}(1+\hat{s})-\lambda)$$

$$+8\hat{m}_\ell^4(6+6\hat{r}_{K_1}^2+3(-2+\hat{s})\hat{s}-6\hat{r}_{K_1}(2+\hat{s})-\lambda)$$

$$-6\hat{m}_\ell^2\hat{s}(1+\hat{r}_{K_1}^2+3(-2+\hat{s})\hat{s}-2(\hat{r}_{K_1}+3\hat{r}_{K_1}\hat{s})-\lambda)\Bigg)\lambda$$

$$-\frac{|\mathcal{E}|^2(3(8\hat{m}_\ell^4+2\hat{m}_\ell^2\hat{s}-\hat{s}^2)\lambda+(8\hat{m}_\ell^4-6\hat{m}_\ell^2\hat{s}+\hat{s}^2)\lambda)}{6\hat{m}_\ell^2}$$

$$+\frac{Re[\mathcal{BC}^*](-1+\hat{r}_{K_1}+\hat{s})(3\hat{s}(2\hat{m}_\ell^2)\lambda-(8\hat{m}_\ell^4-3\hat{m}_\ell^2\hat{s}+\hat{s}^2)\lambda)}{3\hat{m}_\ell^2\hat{r}_{K_1}\hat{s}}$$

$$+\frac{|\mathcal{C}|^2\lambda(3\hat{s}(2\hat{m}_\ell^2+\hat{s})\lambda-(8\hat{m}_\ell^4-2\hat{m}_\ell^2\hat{s}+\hat{s}^2))\lambda}{6\hat{m}_\ell^2\hat{r}_{K_1}\hat{s}}$$

$$+\frac{|\mathcal{A}|^2(-3(8\hat{m}_\ell^4-6\hat{m}_\ell^2\hat{s}+\hat{s}^2)\lambda+(8\hat{m}_\ell^4-2\hat{m}_\ell^2\hat{s}+\hat{s}^2))\lambda}{6\hat{m}_\ell^2}$$

$$+\frac{|\mathcal{F}|^2}{6\hat{m}_\ell^2\hat{r}_{K_1}\hat{s}}\Bigg(6\hat{m}_\ell^2\hat{s}(\hat{r}_{K_1}^2+(-1+\hat{s})^2+\hat{r}_{K_1}(-2+6\hat{s})-\lambda)$$

$$+\hat{s}^2(-3\hat{r}_{K_1}^2-3(-1+\hat{s})^2+6\hat{r}_{K_1}(1+\hat{s})+\lambda)+8\hat{m}_\ell^4(-6(-1+\hat{r}_{K_1}+\hat{s})^2+\lambda)\Bigg)$$

$$+\frac{|\mathcal{B}|^2}{6\hat{m}_\ell^2\hat{r}_{K_1}\hat{s}}\Bigg(\hat{s}^2(3\hat{r}_{K_1}^2+3(-1+\hat{s})^2-6\hat{r}_{K_1}(1+\hat{s})-\lambda)$$

$$-8\hat{m}_\ell^4(12\hat{r}_{K_1}\hat{s}+\lambda)+2\hat{m}_\ell^2\hat{s}(3(\hat{r}_{K_1}^2+(-1+\hat{s})^2+2\hat{r}_{K_1}(-1+7\hat{s}))+\lambda)\Bigg)$$

$$-\frac{Re[\mathcal{FG}^*]}{6\hat{m}_\ell^2\hat{r}_{K_1}\hat{s}}\Bigg(\hat{s}^2(-1+\hat{r}_{K_1}+\hat{s})(3\hat{r}_{K_1}^2+3(-1+\hat{s})^2-6\hat{r}_{K_1}(1+\hat{s})-\lambda)$$

$$+8\hat{m}_\ell^4(6\hat{r}_{K_1}^2-9\hat{r}_{K_1}^2(2+\hat{s})+(-1+\hat{s})(6+3(-3+\hat{s})\hat{s}-\lambda)$$

$$-\hat{r}_{K_1}(-18 + 6\hat{s} + \lambda)) - 6\hat{m}_\ell^2 \hat{s}(\hat{r}_{K_1}^3 + \hat{r}_{K_1}^2(-3 + \hat{s})$$

$$+(-1 + \hat{s})(1 + \hat{s}(-4 + 3\hat{s}) - \lambda) - \hat{r}_{K_1}(-3 + \hat{s}(6 + 5\hat{s}) + \lambda)) \Bigg)$$

$$P_{TT} = \frac{|\mathcal{E}|^2}{3}(4\hat{m}_\ell^2 - \hat{s})(3 + 3\hat{r}_{K_1}^2 - 6\hat{s} + 3\hat{s}^2 - 6\hat{s}(1 + \hat{s}) - 5\lambda)$$

$$-\frac{8Re[\mathcal{FH}^*]\hat{m}_\ell^2 \lambda}{\hat{r}_{K_1}} - \frac{8Re[\mathcal{GH}^*]\hat{m}_\ell^2(-1 + \hat{r}_{K_1})\lambda}{\hat{r}_{K_1}} + \frac{4|\mathcal{H}|^2 \hat{m}_\ell^2 \hat{s}\lambda}{\hat{r}_{K_1}}$$

$$-\frac{2Re[\mathcal{BC}^*](-1 + \hat{r}_{K_1} + \hat{s})}{3\hat{r}_{K_1}\hat{s}}$$

$$\times \Bigg(-6(1 + \hat{r}_{K_1})\hat{s}^2 + 3\hat{s}^2 + \hat{s}(3 - 6\hat{r}_{K_1} + 3\hat{r}_{K_1}^2 - 5\lambda) + 4\hat{m}_\ell^2 \lambda \Bigg)$$

$$-\frac{|\mathcal{C}|^2 \lambda(-6(1 + \hat{r}_{K_1})\hat{s}^2 + 3\hat{s}^2 + \hat{s}(3 - 6\hat{r}_{K_1} + 3\hat{r}_{K_1}^2 - 5\lambda) + 4\hat{m}_\ell^2 \lambda)}{3\hat{r}_{K_1}\hat{s}}$$

$$+\frac{|\mathcal{F}|^2(-6(1 + \hat{r}_{K_1})\hat{s}^2 + 3\hat{s}^2 + \hat{s}(3 - 6\hat{r}_{K_1} + 3\hat{r}_{K_1}^2 - 5\lambda) + 20\hat{m}_\ell^2 \lambda)}{3\hat{r}_{K_1}\hat{s}}$$

$$+\frac{|\mathcal{G}|^2 \lambda}{3\hat{r}_{K_1}\hat{s}} \Bigg(-6(1 + 2\hat{m}_\ell^2 + \hat{r}_{K_1})\hat{s}^2 + 3\hat{s}^3$$

$$+\hat{s}(3 - 6\hat{r}_{K_1} + 3\hat{r}_{K_1}^2 + 24\hat{m}_\ell 62(1 + \hat{r}_{K_1}) - 5\lambda) + 20\hat{m}_\ell^2 \lambda \Bigg)$$

$$+|\mathcal{A}|^2 \Bigg(\frac{\hat{s}}{3}(3 + 3\hat{r}_{K_1}^2 - 6\hat{s} + 3\hat{s}^2 - 6\hat{r}_{K_1}(1 + \hat{s}) - 5\lambda)$$

$$+\hat{m}_\ell^2 \left(-4 - 4\hat{r}_{K_1}^2 + 8\hat{s} - 4\hat{s}^2 + 8\hat{r}_{K_1}(1 + \hat{s}) + \frac{4\lambda}{3} \right) \Bigg)$$

$$+\frac{|\mathcal{B}|^2(6(1 + \hat{r}_{K_1})\hat{s}^2 - 3\hat{s}^3 - 4\hat{m}_\ell^2 \lambda + \hat{s}(-3 + (6 - 48\hat{m}_\ell^2)\hat{r}_{K_1} - 3\hat{r}_{K_1}^2 + 5\lambda))}{3\hat{r}_{K_1}\hat{s}}$$

$$-\frac{2Re[\mathcal{FG}^*]}{3\hat{r}_{K_1}\hat{s}}(3(3 - 4\hat{m}_\ell^2 + \hat{r}_{K_1})\hat{s}^3 - 3\hat{s}^4 + \hat{s}(1 + 4\hat{m}_\ell^2 - \hat{r}_{K_1})$$

$$\times (3 - 6\hat{r}_{K_1} + 3\hat{r}_{K_1}^2 - 5\lambda) - 20\hat{m}_\ell^2(-1 + \hat{r}_{K_1})\lambda + \hat{s}^2$$

$$\times (-9 + 6\hat{r}_{K_1} + 3\hat{r}_{K_1}^2 - 24\hat{m}_\ell^2(1 + \hat{r}_{K_1}) + 5\lambda))$$

$$P_{LT} = -2Re[\mathcal{AF}^* + \mathcal{BE}^*]\pi\hat{m}_\ell v\sqrt{\hat{s}}\lambda - \frac{|\mathcal{F}|^2 \pi\hat{m}_\ell(-1 + \hat{r}_{K_1} + \hat{s})v\sqrt{\lambda}}{\hat{r}_{K_1}\sqrt{\hat{s}}}$$

$$+\frac{Re[\mathcal{FH}^*]\pi\hat{m}_\ell v(-1 + \hat{r}_{K_1} + \hat{s})\sqrt{\hat{s}\lambda}}{\hat{r}_{K_1}}$$

$$+\frac{Re[\mathcal{FG}^*]\pi\hat{m}_\ell(-2 - 2\hat{r}_{K_1}^2 + 3\hat{s} - \hat{s}^2 + \hat{r}_{K_1}(4 + \hat{s}))v\sqrt{\lambda}}{\hat{r}_{K_1}\sqrt{\hat{s}}}$$

$$-\frac{|\mathcal{G}|^2 \pi\hat{m}_\ell(-1 + \hat{r}_{K_1})\lambda^{\frac{3}{2}}}{\hat{r}_{K_1}\sqrt{\hat{s}}} + \frac{Re[\mathcal{GH}^*]\pi\hat{m}_\ell v\lambda^{\frac{3}{2}}\sqrt{\hat{s}}}{\hat{r}_{K_1}}$$

$$P_{TL} = 2Re[\mathcal{AF}^* + \mathcal{BE}^*]\pi\hat{m}_\ell v\sqrt{\hat{s}}\lambda - \frac{|\mathcal{F}|^2\pi\hat{m}_\ell(-1 + \hat{r}_{K_1} + \hat{s})v\sqrt{\lambda}}{\hat{r}_{K_1}\sqrt{\hat{s}}}$$

$$+ \frac{Re[\mathcal{FH}^*]\pi\hat{m}_\ell v(-1 + \hat{r}_{K_1} + \hat{s})\sqrt{\hat{s}\lambda}}{\hat{r}_{K_1}}$$

$$+ \frac{Re[\mathcal{FG}^*]\pi\hat{m}_\ell(-2 - 2\hat{r}_{K_1}^2 + 3\hat{s} - \hat{s}^2 + \hat{r}_{K_1}(4 + \hat{s}))v\sqrt{\lambda}}{\hat{r}_{K_1}\sqrt{\hat{s}}}$$

$$- \frac{|\mathcal{G}|^2\pi\hat{m}_\ell(-1 + \hat{r}_{K_1})\lambda^{\frac{3}{2}}}{\hat{r}_{K_1}\sqrt{\hat{s}}} + \frac{Re[\mathcal{GH}^*]\pi\hat{m}_\ell v\lambda^{\frac{3}{2}}\sqrt{\hat{s}}}{\hat{r}_{K_1}}$$

$$P_{NN} = \frac{1}{3}(|\mathcal{A}|^2 - |\mathcal{E}|^2)(4\hat{m}_\ell^2 - \hat{s})(3 + 3\hat{r}_{K_1}^2 - 6\hat{s} + 3\hat{s}^2 - 6(1 - \hat{s}) - \lambda) + \frac{8Re[\mathcal{FH}^*]\hat{m}_\ell^2\lambda}{\hat{r}_{K_1}}$$

$$+ \frac{8Re[\mathcal{GH}^*]\hat{m}_\ell^2(-1 + \hat{r}_{K_1})\lambda}{\hat{r}_{K_1}} - \frac{4|\mathcal{H}|^2\hat{m}_\ell^2\hat{s}\lambda}{\hat{r}_{K_1}}$$

$$+ \frac{2Re[\mathcal{BC}^*](-1 + \hat{r}_{K_1} + \hat{s})(-6(1 + \hat{r}_{K_1})\hat{s}^2 + 3\hat{s}^2 + \hat{s}(3 - 6\hat{r}_{K_1} + 3\hat{r}_{K_1}^2 - \lambda) + 4\hat{m}_\ell^2\lambda)}{3\hat{s}\hat{r}_{K_1}}$$

$$+ \frac{(|\mathcal{C}|^2 - |\mathcal{F}|^2)\lambda(-6(1 + \hat{r}_{K_1})\hat{s}^2 + 3\hat{s}^2 + \hat{s}(3 - 6\hat{r}_{K_1} + 3\hat{r}_{K_1}^2 - \lambda) - 4\hat{m}_\ell^2\lambda)}{3\hat{s}\hat{r}_{K_1}}$$

$$+ \frac{|\mathcal{B}|^2(-6(1 + \hat{r}_{K_1})\hat{s}^2 + 3\hat{s}^2 + \hat{s}(3 + 6(-1 + 8\hat{m}_\ell^2)\hat{r}_{K_1} + 3\hat{r}_{K_1}^2 - \lambda) + 4\hat{m}_\ell^2\lambda)}{3\hat{s}\hat{r}_{K_1}}$$

$$- \frac{|\mathcal{G}|^2\lambda(-6(1 + \hat{r}_{K_1} + 2\hat{m}_\ell^2)\hat{s}^2 + 3\hat{s}^2 + \hat{s}(3 - 6\hat{r}_{K_1} + 3\hat{r}_{K_1}^2 + 24\hat{m}_\ell^2(1 + \hat{r}_{K_1}) - \lambda) - 4\hat{m}_\ell^2\lambda)}{3\hat{s}\hat{r}_{K_1}}$$

$$+ 2\frac{Re[\mathcal{FG}^*]}{3\hat{r}_{K_1}\hat{s}}\left(3(3 + 4\hat{m}_\ell^2 + \hat{r}_{K_1})\hat{s}^3 - 3\hat{s}^4 + (1 + 4\hat{m}_\ell^2 - \hat{r}_{K_1})\hat{s}(3 - 6\hat{r}_{K_1} + 3\hat{r}_{K_1}^2 - \lambda) \right.$$

$$\left. - 4\hat{m}_\ell^2(-1 + \hat{r}_{K_1})\lambda\hat{s}^2(-9 + 6\hat{r}_{K_1} + 3\hat{r}_{K_1}^2 - 24\hat{m}_\ell^2(1 + \hat{r}_{K_1}) + \lambda) \right)$$

$$P_{LN} = \frac{Im[\mathcal{BF}^*]\pi\hat{m}_\ell(-1 + \hat{r}_{K_1} + \hat{s})v\sqrt{\lambda}}{\hat{r}_{K_1}\sqrt{\hat{s}}}$$

$$+ \frac{Im[\mathcal{BG}^*]\pi\hat{m}_\ell(-1 + \hat{r}_{K_1})(-1 + \hat{r}_{K_1} + \hat{s})\sqrt{\lambda}}{\hat{r}_{K_1}\sqrt{\hat{s}}} - \frac{Im[\mathcal{BH}^*]\pi\hat{m}_\ell(-1 + \hat{r}_{K_1} + \hat{s})v\sqrt{\hat{s}\lambda}}{\hat{r}_{K_1}}$$

$$+ \frac{Im[\mathcal{CF}^*]\pi\hat{m}_\ell\lambda^{\frac{3}{2}}}{\hat{r}_{K_1}\sqrt{\hat{s}}} + \frac{Im[\mathcal{CG}^*]\pi\hat{m}_\ell(-1 + \hat{r}_{K_1})\lambda^{\frac{3}{2}}}{\hat{r}_{K_1}\sqrt{\hat{s}}} - \frac{Im[\mathcal{CH}^*]\pi\hat{m}_\ell\sqrt{\hat{s}}\lambda^{\frac{3}{2}}}{\hat{r}_{K_1}}$$

$$P_{NL} = -\frac{Im[\mathcal{BF}^*]\pi\hat{m}_\ell(-1 + \hat{r}_{K_1} + \hat{s})v\sqrt{\lambda}}{\hat{r}_{K_1}\sqrt{\hat{s}}}$$

$$- \frac{Im[\mathcal{BG}^*]\pi\hat{m}_\ell(-1 + \hat{r}_{K_1})(-1 + \hat{r}_{K_1} + \hat{s})\sqrt{\lambda}}{\hat{r}_{K_1}\sqrt{\hat{s}}} + \frac{Im[\mathcal{BH}^*]\pi\hat{m}_\ell(-1 + \hat{r}_{K_1} + \hat{s})v\sqrt{\hat{s}\lambda}}{\hat{r}_{K_1}}$$

$$- \frac{Im[\mathcal{CF}^*]\pi\hat{m}_\ell\lambda^{\frac{3}{2}}}{\hat{r}_{K_1}\sqrt{\hat{s}}} - \frac{Im[\mathcal{CG}^*]\pi\hat{m}_\ell(-1 + \hat{r}_{K_1})\lambda^{\frac{3}{2}}}{\hat{r}_{K_1}\sqrt{\hat{s}}} + \frac{Im[\mathcal{CH}^*]\pi\hat{m}_\ell\sqrt{\hat{s}}\lambda^{\frac{3}{2}}}{\hat{r}_{K_1}}$$

Parameter	Value
$\alpha_s(m_Z)$	0.119
α_{em}	1/129
$m_{K_1(1270)}$	1.272 (GeV) [24]
$m_{K_1(1400)}$	1.403 (GeV) [24]
$m_{K_{1A}}$	1.31 (GeV) [38]
$m_{K_{1B}}$	1.34 (GeV) [38]
m_b	4.8 (GeV)
m_μ	0.106 (GeV)
m_τ	1.780 (GeV)

Table 3. Input parameters

$$P_{NT} = \frac{4}{3}Im[\mathcal{A}\mathcal{E}^*]\hat{s}v\hat{m}_\ell - 2(Im[\mathcal{B}\mathcal{G}^*] + Im[\mathcal{C}\mathcal{F}^*])$$
$$\frac{v(-1 + \hat{r}_{K_1} + \hat{s})(3 + 3\hat{r}_{K_1}^2 - 6\hat{s} + 3\hat{s}^2 - 6\hat{r}_{K_1}(1 + \hat{s}) - \hat{m}_\ell)}{3\hat{r}_{K_1}}$$
$$-2(Im[\mathcal{C}\mathcal{G}^*]\hat{m}_\ell + Im[\mathcal{B}\mathcal{F}^*])\frac{v(3 + 3\hat{r}_{K_1}^2 - 6\hat{s} + 3\hat{s}^2 - 6\hat{r}_{K_1}(1 + \hat{s}) - \hat{m}_\ell)}{3\hat{r}_{K_1}}$$
$$P_{TN} = -\frac{4}{3}Im[\mathcal{A}\mathcal{E}^*]\hat{s}v\hat{m}_\ell - 2(Im[\mathcal{B}\mathcal{G}^*] + Im[\mathcal{C}\mathcal{F}^*])$$
$$\frac{v(-1 + \hat{r}_{K_1} + \hat{s})(3 + 3\hat{r}_{K_1}^2 - 6\hat{s} + 3\hat{s}^2 - 6\hat{r}_{K_1}(1 + \hat{s}) - \hat{m}_\ell)}{3\hat{r}_{K_1}}$$
$$-2(Im[\mathcal{C}\mathcal{G}^*]\hat{m}_\ell + Im[\mathcal{B}\mathcal{F}^*])\frac{v(3 + 3\hat{r}_{K_1}^2 - 6\hat{s} + 3\hat{s}^2 - 6\hat{r}_{K_1}(1 + \hat{s}) - \hat{m}_\ell)}{3\hat{r}_{K_1}}$$

4 Numerical analysis

Having the explicit expressions for the physically measurable quantities, in this section, we will study the dependence of these quantities on the dileptonic invariant mass(q^2). We will use the parameters given in tables 2 and 4 in our numerical analysis.

We present the dependence of the differential single and double lepton polarization for the $B \to K_1(1272)\ell^+\ell^-$, where $\ell = \mu, \tau$ decay on q^2 as well as its dependence on q^2 due to short distance effects ($\kappa_V \neq 0$ case). The phenomenological factors κ_V for the $B \to K(K^*)\ell^+\ell^-$ decay can be determined from matching the experimental and theoretical results where they supposed to reproduce correct branching ratio relation

$$\mathcal{B}(B \to J/\psi K(K^*) \to K(K^*)\ell^+\ell^-) = \mathcal{B}(B \to J/\psi K(K^*))\mathcal{B}(J/\psi \to \ell^+\ell^-),$$

where the right-hand side is determined from experiments. Using the experimental values of the branching ratios for the $B \to V_i K(K^*)$ and $V_i \to \ell^+\ell^-$ decays, for the lowest two J/ψ and ψ' resonances, the factor κ_V takes the values: $\kappa_V = 2.7$, $\kappa_V = 3.51$ (for K meson), and $\kappa_V = 1.65$, $\kappa_V = 2.36$ (for K^* meson). The values of κ_V used for higher resonances are

usually the average of the values obtained for the J/ψ and ψ' resonances. Using eq. (2.6) and the results for κ_V obtained for $B \to K^*$ transition [10]. We find $\kappa_V = 1.75$ for $J/\Psi(1S)$ and $\kappa_V = 2.43$ for $\Psi(2S)$, respectively.

It is also experimentally useful to consider the averaged values of these asymmetries. Therefore, we shall calculate the averaged values of the polarization asymmetries using the averaging procedure defined as;

$$\langle \mathcal{P} \rangle = \frac{\displaystyle\int_{4\hat{m}_\ell^2}^{(1-\sqrt{\hat{r}_{K_1}})^2} \mathcal{P}\frac{d\mathcal{B}}{d\hat{s}}d\hat{s}}{\displaystyle\int_{4\hat{m}_\ell^2}^{(1-\sqrt{\hat{r}_{K_1}})^2} \frac{d\mathcal{B}}{d\hat{s}}d\hat{s}} \; .$$

, where $\mathcal{B}$ is the branching ratio. The results for averaged value of single and double lepton polarization asymmetries are presented in table 4. Some of these asymmetries in $B \to K_1(1270)\ell^+\ell^-$ decay(i,e., P_{LL}, P_{NN} and P_{TT}) are larger than corresponding asymmetries in $B \to K^*\ell^+\ell^-$ decay presented in ref. [39].

Figures 1–14 show dependence on q^2 when considering the theoretical uncertainties among the formfactors. *Note that, P_N, P_{NL}, P_{LN}, P_{NT} and P_{TN} for μ and τ channels are negligible for all values of q^2. Hence, we do not present their predictions in the figures.*

From these figures, we deduce the following results:

- P_L is plotted in figures 1 and 2 for muon and tau, respectively. It is decreasing for both of muon and and tau channels. Also, its magnitude is much larger for muon channel than tau one. Moreover, there is rather weak dependency on the theoretical uncertainties among the formfactors for tau channel.

- While P_T is decreasing for $q^2 \leq 1.2\text{GeV}^2$ region it is increasing for $q^2 \geq 1.2\text{GeV}^2$ region for muon channel(see figure 3). Its local minimum at the point $q^2 \leq 1.2\text{GeV}^2$ is about -0.15. P_T is increasing in terms of q^2 for tau channel(see figure 4). Also, P_T vanishes at the end of kinematical region for both muon and tau channels.

- P_{LL} takes both negative and positive values depending on q^2. Its zero position occurs at $q^2 \simeq 5\text{GeV}^2$. The measurement of the sign of P_{LL} at $q^2 \leq 8\text{GeV}^2$, which is the nonresonance region, can be used as a good tool to either check the SM prediction or to search for new physics. P_{LL} is quasi uniformly decreasing function of q^2 for tau channel.(see figures 5 and 6). Moreover, there is rather weak dependency on the theoretical uncertainties among the formfactors for tau channel.

- P_{LT} is decreasing for $q^2 \leq 0.8(14.5)\text{GeV}^2$ region but increasing for $q^2 \geq 0.8(14.5)\text{GeV}^2$ region for muon(tau) channel (see figures 7 and 8). Its local minimum at the point $q^2 \leq 0.8(14.5)\text{GeV}^2$ is about $-0.2(0.22)$ for muon(tau) channel, respectively. Also, P_{LT} vanishes at the end of kinematical region for both muon and tau channels. Moreover, there is rather weak dependency on the theoretical uncertainties among the formfactors for tau channel(see figure 8).
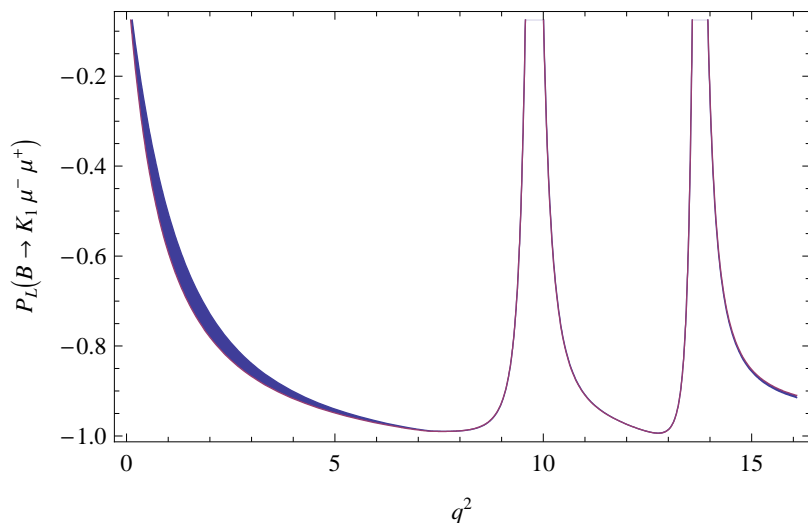
Figure 1. The dependence of the P_L on q^2 for $B \to K_1(1270)\mu^+\mu^-$ decay, where the colored region shows the variation when theoretical uncertainties among the form factors take into account.
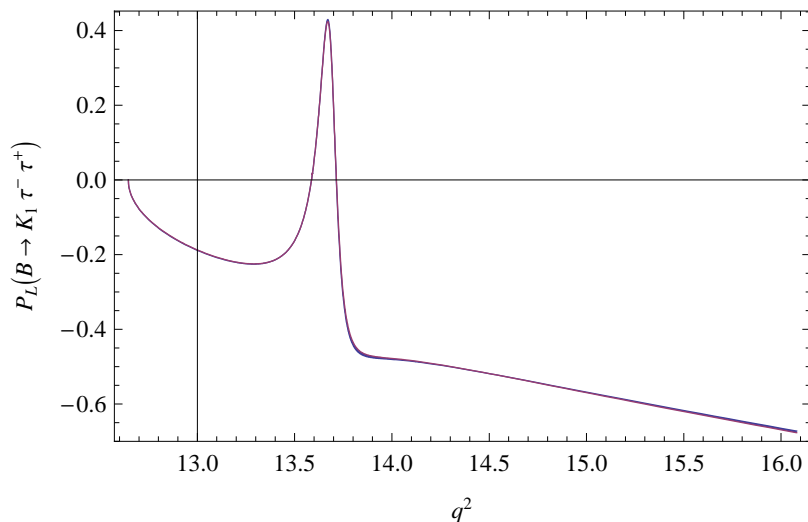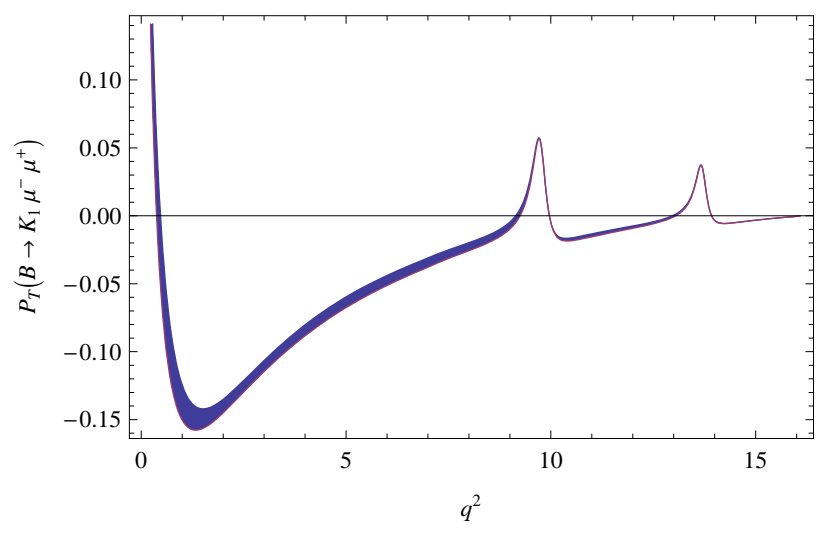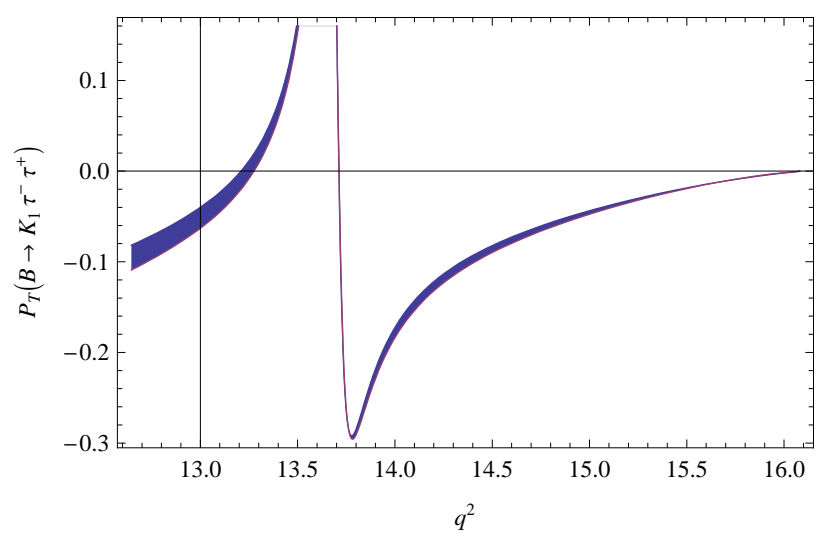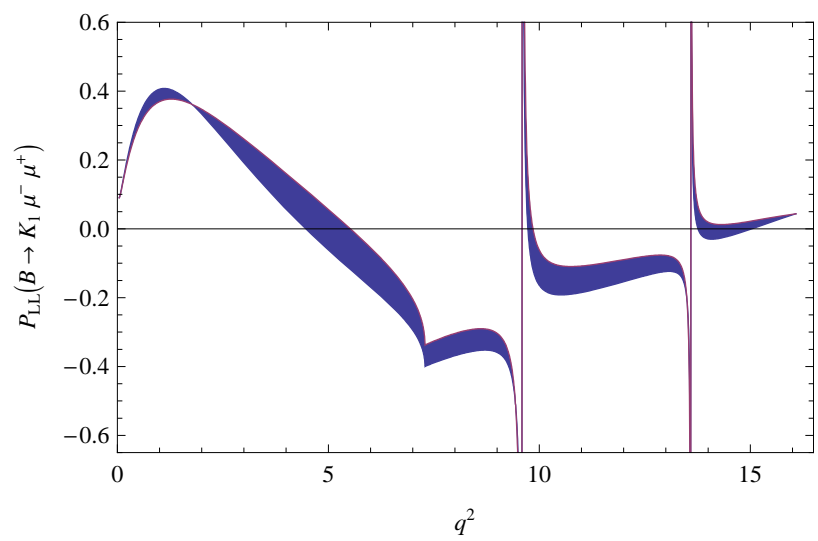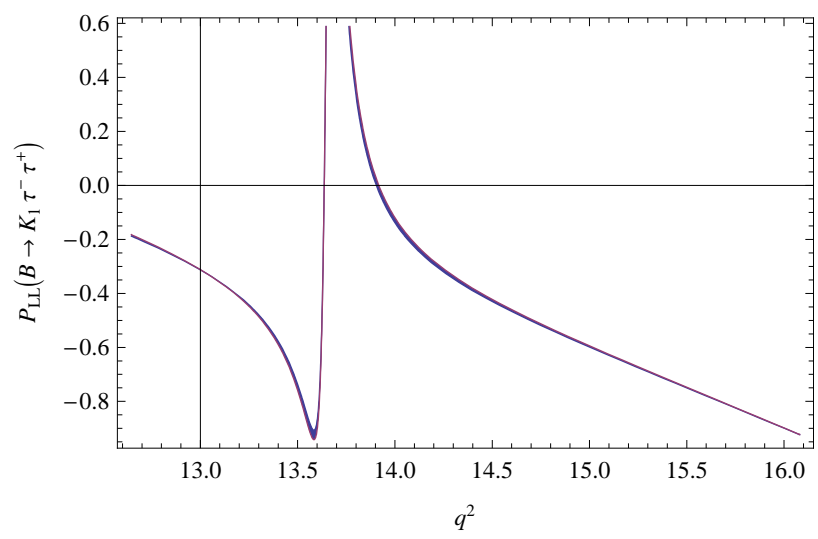

Figure 2. The same as in figure 1, but for the τ lepton.

- P_{NN} and P_{TT} without resonance contributions are negligible at $q^2 \geq 8\text{GeV}^2$ region for muon channel(see figures 9 and 11). P_{TT} takes much larger values in the high q^2 region than the low q^2 region for tau channel (see figure 12).

- P_{TL} is decreasing for $q^2 \leq 0.6\text{GeV}^2$ region but increasing for $q^2 \geq 0.6)\text{GeV}^2$ region for muon channel, (see figure 13). Its local minimum at the point $q^2 \leq 0.6\text{GeV}^2$ is about -0.25. P_{TL} is negligible for all values of q^2 for tau lepton (see figure 14). Also, P_{LT} vanishes at the end of kinematical region for both muon and tau channels.

Figure 3. The dependence of the P_T on q^2 for $B \to K_1(1270)\mu^+\mu^-$ decay, where the colored region shows the variation when theoretical uncertainties among the form factors take into account.
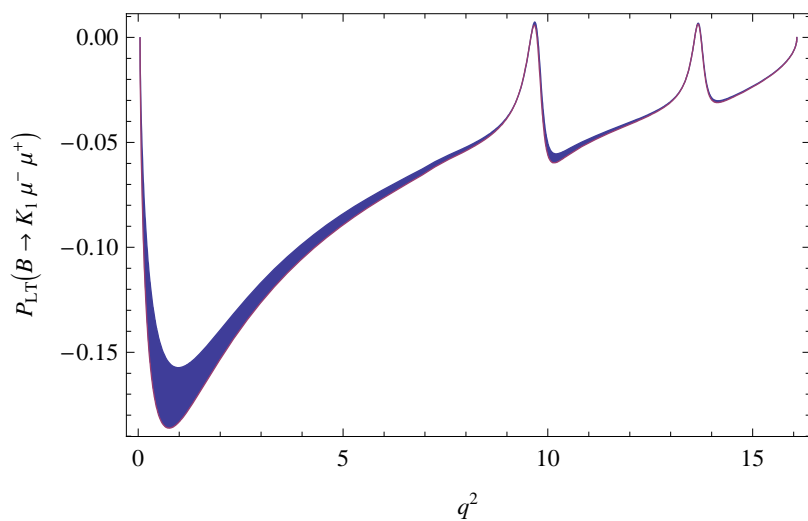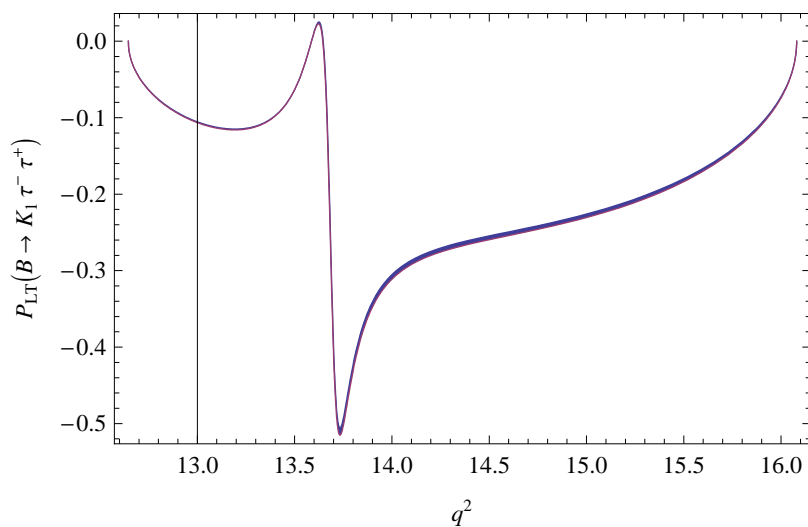

Figure 4. The same as in figure 3, but for the τ lepton.

Figure 5. The dependence of the P_{LL} on q^2 for $B \to K_1(1270)\mu^+\mu^-$ decay, where the colored region shows the variation when theoretical uncertainties among the form factors take into account.
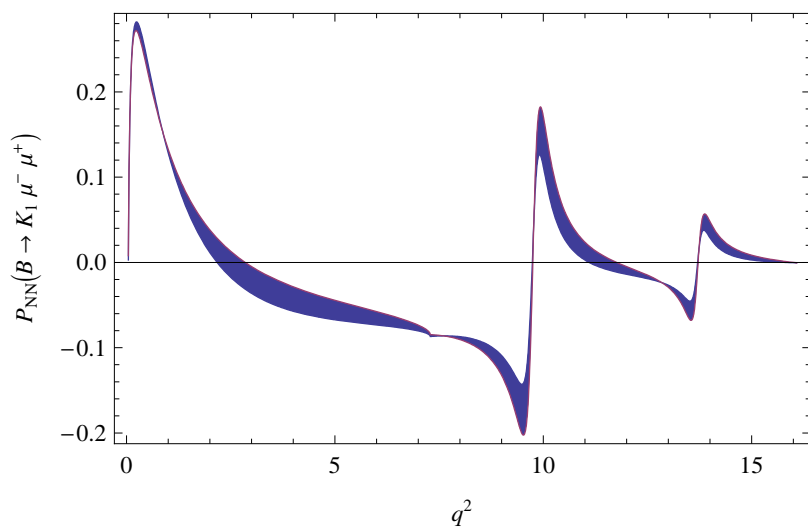

Figure 6. The same as in figure 5, but for the τ lepton.

Figure 7. The dependence of the P_{LT} on q^2 for $B \to K_1(1270)\mu^+\mu^-$ decay, where the colored region shows the variation when theoretical uncertainties among the form factors take into account.
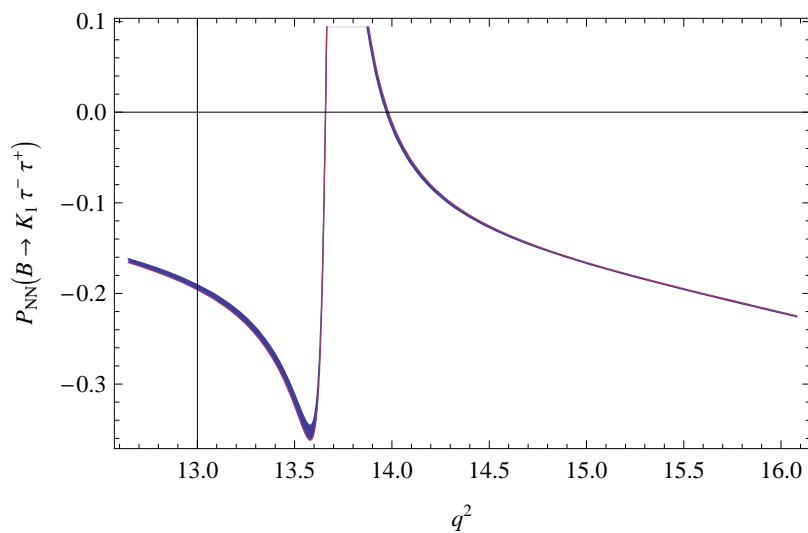

Figure 8. The same as in figure 7, but for the τ lepton.

Figure 9. The dependence of the P_{NN} on q^2 for $B \to K_1(1270)\mu^+\mu^-$ decay, where the colored region shows the variation when theoretical uncertainties among the form factors take into account.
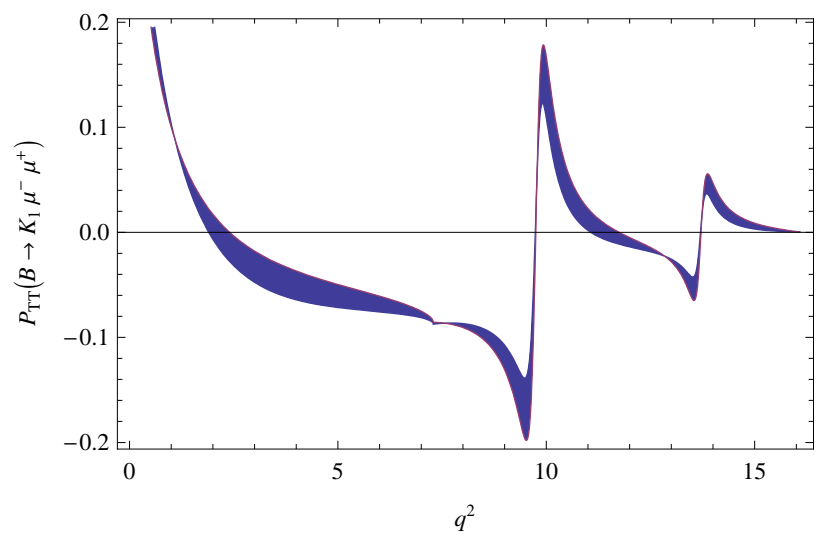

Figure 10. The same as in figure 9, but for the τ lepton.

Figure 11. The dependence of the P_{TT} on q^2 for $B \to K_1(1270)\mu^+\mu^-$ decay, where the colored region shows the variation when theoretical uncertainties among the form factors take into account.
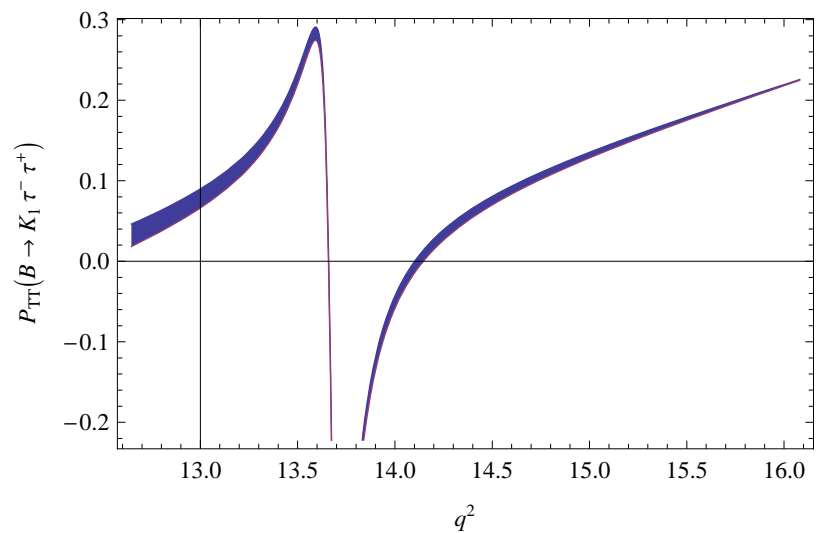

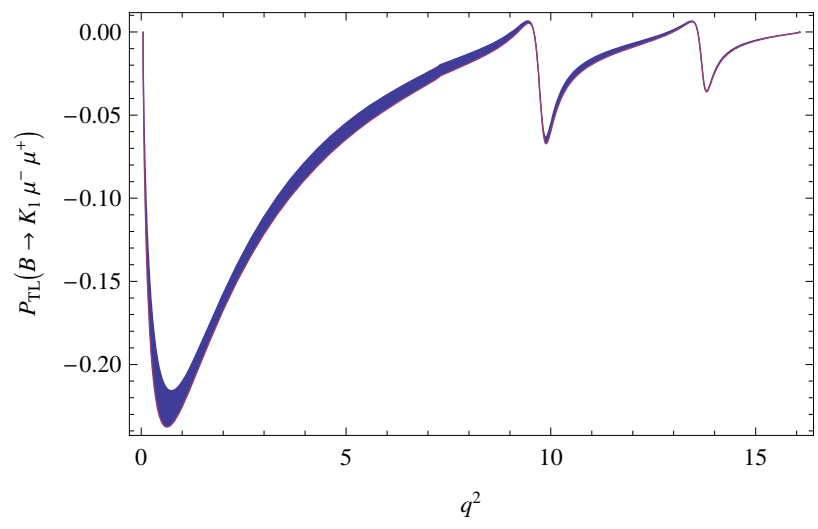**Figure 12**. The same as in figure 11, but for the τ lepton.

Figure 13. The dependence of the P_{TL} on q^2 for $B \to K_1(1270)\mu^+\mu^-$ decay, where the colored region shows the variation when theoretical uncertainties among the form factors take into account.
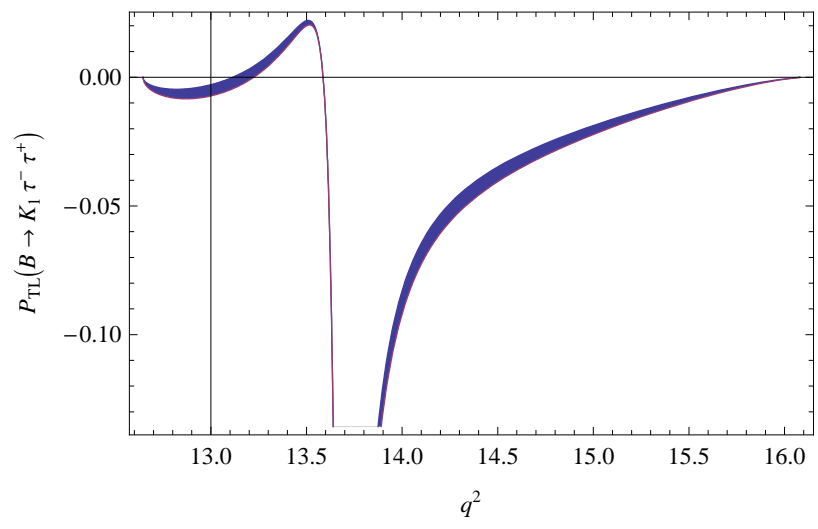

Figure 14. The same as in figure 13, but for the τ lepton.

$\langle P_{ij} \rangle$	$B \to K_1(1272)\mu^+\mu^-$	$B \to K_1(1272)\tau^+\tau^-$
$\langle P_L \rangle$	-0.91 ± 0.006	-0.43 ± 0.001
$\langle P_T \rangle$	-0.016 ± 0.001	-0.05 ± 0.004
$\langle P_N \rangle$	0.001 ± 0.001	0.01 ± 0.001
$\langle P_{LL} \rangle$	-0.34 ± 0.0053	-0.06 ± 0.000
$\langle P_{LN} \rangle$	-0.001 ± 0.000	-0.03 ± 0.001
$\langle P_{NL} \rangle$	0.001 ± 0.000	0.03 ± 0.001
$\langle P_{LT} \rangle$	-0.06 ± 0.003	-0.17 ± 0.000
$\langle P_{TL} \rangle$	-0.03 ± 0.003	-0.01 ± 0.000
$\langle P_{TT} \rangle$	0.015 ± 0.002	0.11 ± 0.002
$\langle P_{NN} \rangle$	0.01 ± 0.004	-0.17 ± 0.001
$\langle P_{NT} \rangle$	-0.006 ± 0.001	0.001 ± 0.001
$\langle P_{TN} \rangle$	0.006 ± 0.001	0.001 ± 0.001

Table 4. Averaged values of single and double lepton polarizations

Finally, the quantitative estimation about the accessibility to measure the various physical observables are in order. An observation of a 3σ signal for asymmetry of the order of the 1% requires about $\sim 10^{12}$ $\bar{B}B$ pairs. The number of $b\bar{b}$ pairs that are produced at B-factories and LHC are about $\sim 5 \times 10^8$ and 10^{12}, respectively. As a result, q^2 dependence of the polarization asymmetries shown by figures 1–13 as well as averaged values of the same asymmetries presented in table 4 can be detectable at LHC. Note that, the ratio of physical observables (for instance, CP , foreward-backward and single or double lepton polarization asymmetries) less suffers from the uncertainty among the formfactors where large parts of the uncertainties partially cancel out.

In conclusion, the single and double lepton polarization asymmetries for exclusive dilepton rare B decays of $B \to K_1(1272)\ell^+\ell^-$ are studied. We have shown that while some components of lepton polarizations are almost zero, some other components are sizable to be measured at the future experiments. Moreover, we show that some of these asymmetries in $B \to K_1(1270)\ell^+\ell^-$ decay(i,e., P_{LL}, P_{NN} and P_{TT}) are larger than corresponding asymmetries in $B \to K^*\ell^+\ell^-$ decay. The study of the magnitude and the size of these physical observables can be used either to probe the predictions of SM or to search for new physics effects.

Acknowledgments

References

[1] BABAR collaboration, B. Aubert et al., *Measurements of branching fractions, rate asymmetries and angular distributions in the rare decays $B \to K\ell^+\ell^-$ and $B \to K^*\ell^+\ell^-$*, *Phys. Rev.* **D 73** (2006) 092001 [hep-ex/0604007] [SPIRES].

[2] BELLE collaboration, A. Ishikawa et al., *Measurement of forward-backward asymmetry and Wilson coefficients in* $B \to K^* \ell^+ \ell^-$, *Phys. Rev. Lett.* **96** (2006) 251801 [hep-ex/0603018] [SPIRES].

[3] BABAR collaboration, B. Aubert et al., *Angular distributions in the decays* $B \to K^* \ell^+ \ell^-$, *Phys. Rev.* **D 79** (2009) 031102 [arXiv:0804.4412] [SPIRES].

[4] BABAR collaboration, B. Aubert et al., *Direct CP, lepton flavor and isospin asymmetries in the decays* $B \to K^{(*)} \ell^+ \ell^-$, *Phys. Rev. Lett.* **102** (2009) 091803 [arXiv:0807.4119] [SPIRES].

[5] G. Eigen, *Exclusive* $b \to s_d \ell\ell$ *decays*, arXiv:0807.4076 [SPIRES].

[6] M.A. Paracha, I. Ahmed and M.J. Aslam, *Form factors, branching ratio and forward-backward asymmetry in* $B \to K_1 \ell^+ \ell^-$ *decays*, *Eur. Phys. J.* **C 52** (2007) 967 [arXiv:0707.0733] [SPIRES].

[7] I. Ahmed, M.A. Paracha and M.J. Aslam, *Exclusive* $B \to K_1 l^+ l^-$ *decay in model with single universal extra dimension*, *Eur. Phys. J.* **C 54** (2008) 591 [arXiv:0802.0740] [SPIRES].

[8] A. Saddique, M.J. Aslam and C.-D. Lu, *Lepton polarization asymmetry and forward backward asymmetry in exclusive* $B \to K_1 \tau^+ \tau^-$ *decay in universal extra dimension scenario*, *Eur. Phys. J.* **C 56** (2008) 267 [arXiv:0803.0192] [SPIRES].

[9] H. Hatanaka and K.-C. Yang, $K_1(1270)$-$K_1(1400)$ *mixing angle and new-physics effects in* $B \to K1 \ell^+ \ell^-$ *decays*, *Phys. Rev.* **D 78** (2008) 074007 [arXiv:0808.3731] [SPIRES].

[10] A. Ali, P. Ball, L.T. Handoko and G. Hiller, *A comparative study of the decays* $B \to (K, K^*) \ell^+ \ell^-$ *in standard model and supersymmetric theories*, *Phys. Rev.* **D 61** (2000) 074024 [hep-ph/9910221] [SPIRES].

[11] A. Ali, E. Lunghi, C. Greub and G. Hiller, *Improved model independent analysis of semileptonic and radiative rare* B *decays*, *Phys. Rev.* **D 66** (2002) 034002 [hep-ph/0112300] [SPIRES].

[12] M. Beneke, T. Feldmann and D. Seidel, *Systematic approach to exclusive* $B \to V \ell^+ \ell^-$, V *gamma decays*, *Nucl. Phys.* **B 612** (2001) 25 [hep-ph/0106067] [SPIRES].

[13] T. Feldmann and J. Matias, *Forward-backward and isospin asymmetry for* $B \to K^* \ell^+ \ell^-$ *decay in the standard model and in supersymmetry*, *JHEP* **01** (2003) 074 [hep-ph/0212158] [SPIRES].

[14] F. Krüger and J. Matias, *Probing new physics via the transverse amplitudes of* $B^0 \to K^{*0}(\to K^- pi^+) \ell^+ \ell^-$ *at large recoil*, *Phys. Rev.* **D 71** (2005) 094009 [hep-ph/0502060] [SPIRES].

[15] C. Bobeth, G. Hiller and G. Piranishvili, *CP asymmetries in bar* $B \to \bar{K}^*(\to \bar{K}\pi)\bar{\ell}\ell$ *and untagged* $\bar{B}_s$, $B_s \to \phi(\to K^+ K^-)\bar{\ell}\ell$ *decays at NLO*, *JHEP* **07** (2008) 106 [arXiv:0805.2525] [SPIRES].

[16] U. Egede, T. Hurth, J. Matias, M. Ramon and W. Reece, *New observables in the decay mode* $\bar{B} \to \bar{K}^{*0} \ell^+ \ell^-$, *JHEP* **11** (2008) 032 [arXiv:0807.2589] [SPIRES].

[17] W. Altmannshofer et al., *Symmetries and asymmetries of* $B \to K^* \mu^+ \mu^-$ *decays in the standard model and beyond*, *JHEP* **01** (2009) 019 [arXiv:0811.1214] [SPIRES].

[18] C.-H. Chen, C.-Q. Geng and L. Li, *New CP phase of* B_s - $\bar{B}_s$ *mixing on T violation in* $B_{d(s)} \to K^*(\phi)\ell^+ \ell^-$, *Phys. Lett.* **B 670** (2009) 374 [arXiv:0808.0127] [SPIRES].

[19] V. Bashiry and K. Zeynali, *Exclusive* $B \to \pi \ell^+ \ell^-$ *and* $B \to \rho \ell^+ \ell^-$ *Decays in the universal extra dimension*, *Phys. Rev.* **D 79** (2009) 033006 [arXiv:0805.3386] [SPIRES].

[20] M. Suzuki, *Strange axial - vector mesons*, *Phys. Rev.* **D 47** (1993) 1252 [SPIRES].

[21] L. Burakovsky and J.T. Goldman, *Towards resolution of the enigmas of P-wave meson spectroscopy*, *Phys. Rev.* **D 57** (1998) 2879 [hep-ph/9703271] [SPIRES].

[22] H.-Y. Cheng, *Hadronic charmed meson decays involving axial vector mesons*, *Phys. Rev.* **D 67** (2003) 094007 [hep-ph/0301198] [SPIRES].

[23] H. Hatanaka and K.-C. Yang, *B → K₁γ decays in the light-cone QCD sum rules*, *Phys. Rev.* **D 77** (2008) 094023 [*Erratum ibid.* **D 78** (2008) 059902] [arXiv:0804.3198] [SPIRES].

[24] PARTICLE DATA GROUP collaboration, C. Amsler et al., *Review of particle physics*, *Phys. Lett.* **B 667** (2008) 1 [SPIRES].

[25] A.J. Buras and M. Münz, *Effective Hamiltonian for B → Xₛe⁺e⁻ beyond leading logarithms in the NDR and HV schemes*, *Phys. Rev.* **D 52** (1995) 186 [hep-ph/9501281] [SPIRES].

[26] C.S. Lim, T. Morozumi and A.I. Sanda, *A prediction for dγ(b → sℓℓ̄)/dQ² including the long distance effects*, *Phys. Lett.* **B 218** (1989) 343 [SPIRES].

[27] W.-S. Hou, R.S. Willey and A. Soni, *Implications of a heavy top quark and a fourth generation on the decays B → Kℓ⁺ℓ⁻, Kνν̄*, *Phys. Rev. Lett.* **58** (1987) 1608 [*Erratum ibid.* **60** (1988) 2337] [SPIRES].

[28] N.G. Deshpande and J. Trampetic, *Improved estimates for processes b → sℓ⁺ℓ⁻, B → Kℓ⁺ℓ⁻ and B → K*ℓ⁺ℓ⁻*, *Phys. Rev. Lett.* **60** (1988) 2583 [SPIRES].

[29] M. Jezabek and J.H. Kuhn, *Lepton spectra from heavy quark decay*, *Nucl. Phys.* **B 320** (1989) 20 [SPIRES].

[30] M. Misiak, *The b → se⁺e⁻ and b → sγ decays with next-to-leading logarithmic QCD corrections*, *Nucl. Phys.* **B 393** 1993 23 [SPIRES].

[31] M. Misiak, *Erratum*, *Nucl. Phys.* **B 439** (1995) 461 [SPIRES].

[32] T. Huber, E. Lunghi, M. Misiak and D. Wyler, *Electromagnetic logarithms in anti-B → X/s ℓ⁺ℓ⁻*, *Nucl. Phys.* **B 740** (2006) 105 [hep-ph/0512066] [SPIRES].

[33] A. Ali, T. Mannel and T. Morozumi, *Forward backward asymmetry of dilepton angular distribution in the decay b → s ℓ⁺ℓ⁻*, *Phys. Lett.* **B 273** (1991) 505 [SPIRES].

[34] F. Krüger and L.M. Sehgal, *Lepton polarization in the decays B → Xₛμ⁺μ⁻ and B → Xₛτ⁺τ⁻*, *Phys. Lett.* **B 380** (1996) 199 [hep-ph/9603237] [SPIRES].

[35] G. Nardulli and T.N. Pham, *B → K₁γ and tests of factorization for two-body non leptonic B decays with axial-vector mesons*, *Phys. Lett.* **B 623** (2005) 65 [hep-ph/0505048] [SPIRES].

[36] K.-C. Yang, *Form factors of B_{u,d,s} decays into P-wave axial-vector mesons in the light-cone sum rule approach*, *Phys. Rev.* **D 78** (2008) 034018 [arXiv:0807.1171] [SPIRES].

[37] S. Fukae, C.S. Kim and T. Yoshikawa, *A systematic analysis of the lepton polarization asymmetries in the rare B decay, B → Xₛτ⁺τ⁻*, *Phys. Rev.* **D 61** (2000) 074015 [hep-ph/9908229] [SPIRES].

[38] K.-C. Yang, *Light-cone distribution amplitudes of axial-vector mesons*, *Nucl. Phys.* **B 776** (2007) 187 [arXiv:0705.0692] [SPIRES].

[39] A.S. Cornell and N. Gaur, *Lepton polarization asymmetries for B → K*ℓ⁺ℓ⁻: a model independent approach*, *JHEP* **02** (2005) 005 [hep-ph/0408164] [SPIRES].